

Effects of recycled tyre rubber and steel fibre on the impact resistance of slag-based self-compacting alkali-activated concrete

Anıl Niş, Necip Altay Eren & Abdulkadir Çevik

To cite this article: Anıl Niş, Necip Altay Eren & Abdulkadir Çevik (2023) Effects of recycled tyre rubber and steel fibre on the impact resistance of slag-based self-compacting alkali-activated concrete, European Journal of Environmental and Civil Engineering, 27:1, 519-537, DOI: [10.1080/19648189.2022.2052967](https://doi.org/10.1080/19648189.2022.2052967)

To link to this article: <https://doi.org/10.1080/19648189.2022.2052967>



Published online: 28 Mar 2022.



Submit your article to this journal [↗](#)



Article views: 349



View related articles [↗](#)



View Crossmark data [↗](#)



Citing articles: 3 View citing articles [↗](#)



Effects of recycled tyre rubber and steel fibre on the impact resistance of slag-based self-compacting alkali-activated concrete

Anıl Niş^a, Necip Altay Eren^b and Abdulkadir Çevik^b

^aDepartment of Civil Engineering, Istanbul Gelisim University, Istanbul, Turkey; ^bDepartment of Civil Engineering, Gaziantep University, Gaziantep, Turkey

ABSTRACT

Accumulation of waste tyres causes an environmental disaster because of the rapid rise in transport vehicle demand resulting from modern developments, Covid-19 and similar pandemics. Thus, recycling waste tyres in the form of aggregates as a sustainable construction material can be a solution to reduce the environmental problems. Current research focuses on the impact resistance and mechanical properties of the crumb rubber self-compacting alkali-activated concrete reinforced with 1% steel fibres (SFs) where fine and coarse crumb rubbers (CR) are partially replaced with 10% and 15% replacement ratios. The compressive, flexural, splitting tensile strengths and modulus of elasticity were investigated; impact resistance was found using a drop hammer impact test. The incorporation of CR reduced the mechanical properties, and the reduction was found more with increased rubber contents, whereas the incorporation of SF compensated for the strength loss. The impact performance was enhanced with the CR and SF incorporations. The 15% CR incorporation improved the impact energy up to three times, whereas both 1% SF and 15% CR incorporations significantly enhanced the impact energy up to 30 times. Similar mechanical strengths were obtained for the different sizes of CR. However, impact performance was significantly influenced by the sizes of CR.

ARTICLE HISTORY

Received 13 September 2021
Accepted 2 March 2022

KEYWORDS

Impact energy; self-compacting alkali-activated concrete; impact performance; crumb rubber; drop-weight test; impact resistance

1. Introduction

The transport vehicle demand will increase in the future due to the Covid-19 and related pandemics, which causes an increased number of discarded rubber tyres. More than 500 million worn-out wheels are thrown away or burned without any other use every year (Thomas & Gupta, 2016), a very serious danger to the society and environment, e.g. soil and water pollution during the burning process, and decreased biodiversity resulting from the oil-containing toxics and soluble component of rubber tyres (Chen et al., 2007; Day et al., 1993; Pacheco-Torgal et al., 2012). It is estimated that the amount of waste tyres will climb to ~5000 million in 2030 if the motor vehicle numbers rise to 1200 million (Pacheco-Torgal et al., 2012), which can pose an ecological damage. Also, less usable landfill and increased cost of accumulating and transporting waste tyres are regarded as a significant issue of waste tyre disposal. Therefore, legislations have been introduced by some countries to ban waste tyre disposal in landfills and promote the reutilisation of waste tyres in different applications (Abdelmonem et al., 2019; Raffoul et al., 2016). The potential problems, as well as restricted legislation of waste tyre disposal, encouraged researchers to reuse waste tyre rubbers in concrete as a replacement of natural aggregate, resulting in a sustainable

and greener solution for the environment. Recently, rubberised concrete takes great attention in structural applications due to its environmentally-friendly nature.

Ordinary portland cement (OPC) is an excellent binder material; however, high energy requirement and the released CO₂ during cement production are significant trouble for cement manufacturer, the environment and human being (Alzeebaree et al., 2018). Also, OPC production causes the overutilisation of natural resources, particularly limestone quarries. All the aforementioned key factors encourage researchers to investigate and to develop novel construction materials for reduced cost and lowered environmental hazard (Aly et al., 2019). Recently, an environmentally-friendly geopolymer concrete (GPC) emerges as an alternative to OPC concrete and GPC use as an appropriate aluminosilicate source such as ground-granulated blast furnace slag instead of OPC (Kurtoglu et al., 2018; Niş & Altundal, 2019). Research showed that GPC performed better resistance against creep, shrinkage and chemical attacks (Davidovits, 1994; Wallah & Rangan, 2006) compared to OPC concrete. GPC is an alkali-activated concrete (AAC) and composes of alumina-silicate-based materials (slag and fly ash) and alkali activators and the most commonly utilised one is the combination of sodium silicate and sodium hydroxide for geopolymerisation (Alzeebaree et al., 2020; Çevik et al., 2018). The utilisation of industrial by-product material makes AAC more popular in the concrete industry due to the less environmental impact resulting from reduced CO₂ releases.

Numerous studies have been realised on crumb rubber incorporations into concrete mixes (Eisa et al., 2020; Liu et al., 2016; Youssf et al., 2014). Crumb rubber is a waste tyre material that the size of the whole tyre is decreased and ground into smaller particles ranging from 4.75 mm to 75 µm (Alam et al., 2015). It was reported that crumb rubbers with particle sizes between 1 mm to 4 mm exhibited acceptable mechanical properties for concretes (Bing & Ning, 2014) and the crumb rubber utilisation as fine aggregates performed better mechanical performance than the chip rubber utilisation as coarse aggregates (Alam et al., 2015). In general, crumb rubber replacements as coarse or fine aggregates in concrete decreases compressive strength, splitting tensile strength, elasticity modulus and flexural strength depending on the size and volume ratio of the crumb rubbers (Abdelmonem et al., 2019; Dehdezi et al., 2015; Park et al., 2016; Raffoul et al., 2016; Wongsu et al., 2018; Zheng et al., 2008) whereas increases ductility, fracture toughness and impact resistance of concrete (Gupta et al., 2015; Li et al., 2019; Liu et al., 2012). However, it was reported that the energy absorbing capacity was enhanced with the enhancement of rubber contents up to 10%, while it decreased when the rubber content was more than 10% (Liu et al., 2012), and the suggested maximum rubber content was reported as 20% due to the low mechanical strength reductions in another investigation (Khatib & Bayomy, 1999). Another problem for the rubberised concrete is the premature cracking due to insufficient bonding between rubbers and concrete matrix, so rubberised concrete is suggested to use only non-structural applications (Chan et al., 2019; Ganjian et al., 2009). These weaknesses can be mitigated by using steel fibres (SF) that can increase the mechanical properties (Eisa et al., 2020).

One of the drawbacks of rubberised concrete is the decreased workability due to rubber incorporations. It was reported that the workability significantly decreases when the rubber content exceeds the replacement level by 15% (Siddika et al., 2019). Therefore, the maximum crumb rubber volume was chosen to be 15% in this study. Self-compacting concrete (SCC) could provide a solution to decreased workability as well as good mechanical performances and durability (AbdelAleem et al., 2018; Ma et al., 2017). Also, it was reported that the optimum SF volume ratio was found as 1% considering the fresh state properties of SCC (Niş, 2018; Niş et al., 2020). Therefore, SF content was selected as 1% in this research.

In recent years, structures can expose to impact loadings that may be resulted from several reasons such as collisions, car crash or terrorist attack (Yıldırım et al., 2020). Thus, structural buildings should be able to resist the impact loadings as well as other types of loadings. During impact loadings, structural elements have to absorb huge energy in a very short time. Therefore, primary expectations due to the impact loadings are enhanced ductility and energy absorption capacity. However, OPC or AAC has a brittle material; therefore, the combined use of tyre rubber and SF can be a solution to obtain a more ductile concrete with high energy absorption capacity.

Limited researches have been realised on the impact resistance of crumb rubbers on AAC. The limited research available on the mechanical performance of crumb rubber AAC still leaves things unclear and further researches are required to verify the possible utilisation of crumb rubber AAC where crumb rubbers can be utilised as partial replacements of fine and coarse aggregates (Aly et al., 2019). Also, the combined influences of crumb rubbers and SF on the performances of AAC have not been investigated yet, and it still needs further investigations (Eisa et al., 2020). Current article presents an experimental

study on the fresh and hardened state properties of crumb rubber slag-based self-compacting AAC reinforced with 1% SF considering different crumb rubbers at varying replacement ratios (10% and 15% by volume of aggregates). In addition, there is no study found on the impact performance of crumb rubber slag-based self-compacting AAC reinforced with SF. For the first time, the impact performances of different rubberised SF-reinforced self-compacting AAC was studied herein in details.

2. Experimental methods

2.1. Materials

The ground granulated blast furnace slag (GGBFS) with a specific gravity of 2.70 g/cm^3 and a specific surface area of $418\text{ m}^2/\text{kg}$ was used as a binder for the production of self-compacted alkali-activated concretes (SCAAC). Table 1 indicates the chemical and physical properties of the ground granulated blast furnace slag.

The crushed limestone aggregates were used in the SCC mixtures, and their properties are shown in Table 2. The recycled tyre rubber materials as shown in Figure 1 were replaced with aggregates. Tyre crumb rubber (TCR) was replaced with 10% and 15% of coarse aggregates, and coarse crumb rubber (CCR) and fine crumb rubber (FCR) was replaced with 10% and 15% of fine aggregates. The CCR and FCR were replaced by equal proportions of 5% and 5% (for 10% replacements) or 7.5% and 7.5% (for 15% replacements) with fine aggregates. Table 2 presents the characteristics of crushed limestone aggregates and TCR, CRC and FCR materials. The FCR, CCR and TCR sizes mostly range from 0.25 to 1 mm, 1 to 2 mm, and 2 to 4 mm, respectively.

The SCAAC mixes were produced with using alkali activators, which were composed of a mixing of sodium silicate (water: 55.9%, SiO_2 : 29.4% and Na_2O : 13.7% by weight) and sodium hydroxide (98% purity) having a silicate/hydroxide ratio of 2.5. In a previous study, the $\text{Na}_2\text{SiO}_3/\text{NaOH}$ ratio should be in the range of 1.5–2.5 for economic efficiency (Olivia & Nikraz, 2012); thus, it was chosen as 2.5 in this study. The molarity of NaOH was chosen to be 12 M, which exhibited the superior performance (Alzebaree et al., 2021). In a research, the performance of hooked end SF, corrugated SF and straight SF were evaluated, and hooked-end ones showed superior performance (Wu et al., 2016). Thus, Kemerix 30/40

Table 1. Chemical and physical characteristic of GGBFS.

Component	CaO	SiO ₂	Al ₂ O ₃	Fe ₂ O ₃	MgO	SO ₃	K ₂ O	Na ₂ O	LOI	SG	BF (m ² /kg)
GGBFS (%)	34.12	36.40	11.39	1.69	10.30	0.49	3.63	0.35	1.64	2.79	418

Table 2. The sieve analyses and characteristics of fine and coarse aggregates and waste tyre rubbers.

Materials	Sieve size (mm)							Fineness modulus	Specific gravity	Water (%) absorption
	0.25	0.5	1	2	4	8	16			
Fine aggregate	16.4	28.4	59.9	89.3	100	100	100	2.57	2.45	1.5
Coarse aggregate	0.4	0.5	0.5	0.5	1	31.5	100	5.66	2.72	2.4
Coarse crumb rubber	12.2	21.8	33.5	81.7	100	100	100	2.23	0.83	2.2
Fine crumb rubber	11.1	47.4	86.3	100	100	100	100	1.97	0.48	1.8
Tyre crumb rubber	5.3	9.6	24.6	53.8	89.6	100	100	3.88	1.02	2.9



Fine Crumb Rubber (FCR)



Coarse Crumb Rubber (CCR)



Tyre Crumb Rubber (TCR)

Figure 1. Recycled rubber particles.

Table 3. Components of rubberised mixtures.

Mixture	SF (kg/m ³)	FCR (kg/m ³)	CCR (kg/m ³)	TCR (kg/m ³)	Fine aggregates (kg/m ³)	Coarse aggregates (kg/m ³)	Na ₂ SO ₃ + NaOH (kg/m ³)	SP (%)	Extra water (%)	Slag (kg/m ³)
GB	500	0	0	0	0	860.07	738.12	250	7	10
GB-FCR/5.0-CCR/5.0	500	0	7.95	10.65	0	780.44	738.12	250	7	10
GB-FCR/7.5-CCR/7.5	500	0	11.9	15.98	0	700.80	738.12	250	7	10
GB-TCR/10	500	0	0	0	30.9	621.16	738.12	250	7	10
GB-TCR/15	500	0	0	0	46.36	541.53	738.12	250	7	10
GB-SF/1.0-FCR/5.0-CCR/5.0	500	78.4	7.95	10.65	0	779.00	736.76	250	7	10
GB-SF/1.0-FCR/7.5-CCR/7.5	500	78.4	11.9	15.98	0	699.51	736.76	250	7	10
GB-SF/1.0-TCR/10	500	78.4	0	0	30.9	620.02	736.76	250	7	10
GB-SF/1.0-TCR/15	500	78.4	0	0	46.36	540.53	736.76	250	7	10

hooked-end SF with a diameter of 0.75, an aspect ratio of 40, a length of 30 mm and a fibre fraction of 1% were utilised in this study. In addition, a polycarboxylate ether-based superplasticizer, Master Glenium RMC-303, was utilised to meet the SCC necessities.

2.2. Mixture designs

In this study, recycled tyre rubber (RTR) incorporated nine mixtures in two series were designed and produced. One of them was only containing recycled tyre rubber (10% and 15%), the other containing RTR (10% and 15%) and SF (1%). Table 3 indicated the amount of each component of the mixes. In Table 3, GB represents the reference binder, and FCR, CCR, TCR and SF indicated fine crumb rubber, coarse crumb rubber, tyre crumb rubber and SF, respectively.

For the mixing procedure, binder and aggregates were first mixed dry for 2.5 min. The alkaline activator, extra water and SP were added to the dry mixture within 1 min and mixed for another 2 min. Subsequently, rubbers with/without SF were added and the mixture was mixed for an additional 3 min. The mixes were cast into 100 × 100 × 500 mm prismatic sections for the flexural strength and impact experiments, 100 × 100 × 100 mm cube molds for compressive strengths, and 100 × 200 mm cylinder molds for splitting tensile strengths and elasticity modulus tests. Then, the upper surfaces of the specimens were coated using a plastic sheet to prevent the alkali activators from evaporation. After 24 h, the samples were demoulded and kept in an ambient condition at 23 ± 2 °C for 28 days. The previous study stated that slag incorporated geopolymer/alkali-activated concretes can be used in structures without the need of water-curing and oven-curing (Niş & Altındal, 2021). Thus, curing conditions were not applied and specimens were left in an ambient environment.

2.3. Fresh state properties

The SCC requirements of the rubberised mixes were assessed via slump flow, V-funnel and L-Box tests. The viscosity and flowability were assessed by slump flows and V-funnels, and passing ability was assessed via L-Box tests. The fresh state test procedures were explained in earlier investigations (Gülşan et al., 2019; Niş et al., 2020).

2.4. Drop-weight test

Figure 2 presents the drop-weight test equipment and crack width measurement. The drop-weight tests were realised in accordance with the recommendations of ACI Committee 544 and the test was conducted as repeated impact drops to the same point. In general, a drop-hammer impacted periodically to the mid-point of SCAAC beams at certain drop heights and positions.

For this aim, the prismatic beam samples of 100 × 100 × 500 mm were produced to investigate the impact behavior. The 28.5 kg impactor mass was left to drop from 10 cm height on the mid-point of prismatic beams. For these experiments, acceleration versus time, displacement–time, force–time, and crack formation data were taken at the same time by a load cell to reach load data, and two potentiometers to obtain perpendicular displacement data and two accelerometers to obtain acceleration data and crack

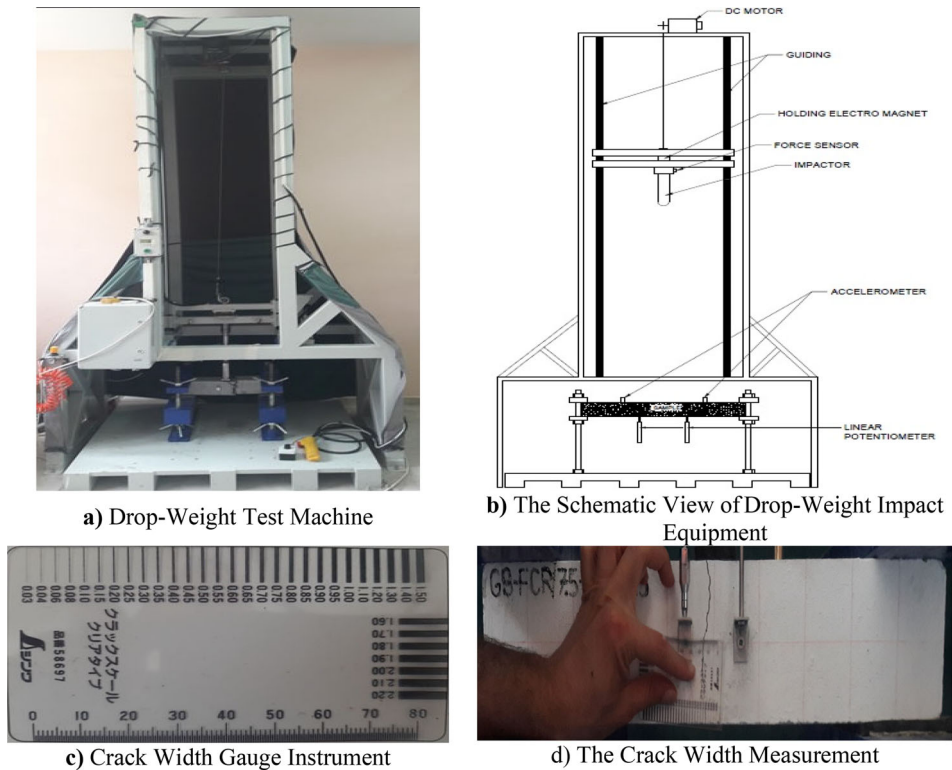


Figure 2. Drop-weight impact test set-up.

width gauge instrument to obtain crack width data were used. The total blow numbers leading to the failure was utilised to reach the failure impact energy using the following formula:

$$E_{\text{impact}}: m \times N \times h \times g$$

where, h = fall height (10 cm), N = blow numbers, $g = 9.81 \text{ m/s}^2$, m = hammer mass (28.5 kg), and E_{impact} = impact energy (Joule).

There are no available guidelines/standards for the flexural impact test. Zhang et al. evaluated various drop heights and weights utilised, and stated that variations of both drop weights and heights considerably changed the impact performances, although the specimen failures are quite different. They reported that drop weights and heights should be selected cautiously (Zhang et al., 2017). In this study, a drop height of 10 cm was selected after preliminary experiments, which was the lowest free-fall height to take sensitive drop numbers. A specific mechanism was designed to hinder rebound after each impacts in the machine. This specific mechanism has photocell sensors that start air compressors, which catches the impactor after first drops and prevents the rebounds. The first cracking in the samples can be understood when an abrupt changes or signs were obtained on the strains, showing visible cracks on the surfaces. Similar experimental procedure about the impact testing is applied in another investigation as reported (Niş et al., 2021). The specimen failure emerges after the breaking of the bond between matrix and SF, leading to the failure of prismatic beams. It should be noted that the precisely generated strain rate measurements of the tested samples under drop-weight impact loads are difficult due to the extremely short duration of the failure process (Gong et al., 2018).

3. Results and discussions

3.1. The fresh state results of SCAAC mixes

Table 4 shows the fresh state results of SCC mixtures. All slump flows were found more than the lowest slump flows of 550 mm by EFNARC committee and 600 mm by EN 12350-8 standards. In addition, T_{50}

Table 4. The fresh state performances.

Samples	L-Box (PL)	V-Funnel (s)	T_{50} (s)	S-Flows (mm)
GB	741 (± 3)	1.00 (± 0)	10.71 (± 0.55)	2.46 (± 0.04)
GB-FCR/5.0-CCR/5.0	704 (± 4)	0.94 (± 0.01)	14.23 (± 0.76)	3.25 (± 0.06)
GB-FCR/7.5-CCR/7.5	673 (± 5)	0.89 (± 0.02)	17.93 (± 0.82)	3.63 (± 0.08)
GB-TCR/10	683 (± 4)	0.90 (± 0.01)	19.49 (± 0.86)	3.47 (± 0.08)
GB-TCR/15	667 (± 6)	0.84 (± 0.02)	22.94 (± 0.94)	3.91 (± 0.11)
GB-SF/1.0-FCR/5.0-CCR/5.0	678 (± 6)	0.90 (± 0.02)	17.57 (± 1.02)	3.37 (± 0.11)
GB-SF/1.0-FCR/7.5-CCR/7.5	664 (± 8)	0.84 (± 0.03)	19.97 (± 1.15)	3.87 (± 0.13)
GB-SF/1.0-TCR/10	672 (± 8)	0.85 (± 0.02)	22.68 (± 1.23)	3.73 (± 0.12)
GB-SF/1.0-TCR/15	657 (± 10)	0.80 (± 0.03)	24.13 (± 1.38)	4.01 (± 0.14)

Table 5. The hardened state properties.

Specimen	Cube compressive strength (MPa)	Modulus of elasticity (GPa)	Splitting tensile strength (MPa)	Flexural strength (MPa)
GB	60.95 (± 0.95)	20.73 (± 0.79)	3.43 (± 0.54)	3.89 (± 0.47)
GB-FCR/5.0-CCR/5.0	52.74 (± 0.86)	19.17 (± 0.67)	3.17 (± 0.45)	3.49 (± 0.43)
GB-FCR/7.5-CCR/7.5	50.74 (± 0.83)	18.47 (± 0.68)	2.97 (± 0.46)	3.35 (± 0.41)
GB-TCR/10	53.23 (± 0.77)	19.52 (± 0.61)	3.12 (± 0.38)	3.61 (± 0.41)
GB-TCR/15	49.31 (± 0.71)	19.18 (± 0.57)	3.02 (± 0.44)	3.49 (± 0.39)
GB-SF/1.0-FCR/5.0-CCR/5.0	55.32 (± 0.63)	21.97 (± 0.54)	3.95 (± 0.41)	4.07 (± 0.37)
GB-SF/1.0-FCR/7.5-CCR/7.5	52.23 (± 0.54)	22.87 (± 0.49)	4.61 (± 0.36)	4.10 (± 0.39)
GB-SF/1.0-TCR/10	56.29 (± 0.64)	22.26 (± 0.43)	4.22 (± 0.38)	4.06 (± 0.38)
GB-SF/1.0-TCR/15	52.85 (± 0.69)	23.19 (± 0.52)	4.65 (± 0.33)	4.11 (± 0.34)

values were found less than the highest recommended T_{50} flow time of 6 s according to EN 12350-8 standard. The results revealed that the mixes had satisfactory flowability. The V-Funnel discharge duration should be lower than 15 s to achieve excellent filling ability according to EN 12350-9 standard. The discharge durations of reference mix and GB-FCR/5.0-CCR/5.0 were found less than 15 s; however, the discharge periods of the other mixes were found higher than 15 s without blocking. It is reminded that SCC test criteria were prepared based on the mixtures without fibres, and still, there are no standards/guidelines existing for the mixtures with fibres. The L-Box tests assess the passing ability by tight spacings (41 ± 1 mm). EN 12350-10 standards and EFNARC guideline/specification recommend that PL values should be higher than the 0.8 to satisfy passing ability criteria. The PL values were found higher than 0.8, implying satisfactory passing ability. The fresh state results revealed that all SCAAC mixtures incorporating rubbers satisfied the flowability and passing ability.

The results revealed a reduction in the flowability and passing ability with an increase in the crumb rubber percentage. The loss in the flowability is less than 10% for all crumb rubber replacements. Similar results were obtained in earlier studies (Abdelmonem et al., 2019; Siddika et al., 2019). In addition, crumb rubbers with larger sizes decreased the flowability and passing ability further due to the increase in friction between the angular rubber particles. Similar findings were also reported in the previous investigations (Holmes et al., 2014; Reda Taha et al., 2008). Moreover, SF incorporation reduced the flowability and passing ability further due to the increased shear resistance with relatively higher viscosity as similar to earlier findings (Eisa et al., 2020; Zhong et al., 2019). The highest decrease in flowability and passing ability was obtained in the mixes including 1% SF and 15% tyre crumb rubbers. The impacts of rubbers and SFs on the fresh state parameters were given in the previous research (Alzebaree et al., 2021).

3.2. The hardened state performances

Table 5 demonstrates the hardened state properties of the SCAAC samples. The compressive strength, splitting tensile strength, modulus of elasticity and flexural strength results were found reduced with an increase in the crumb rubber content. The reduction in mechanical strengths due to the increase in the rubber percentages were also reported in earlier investigations (Atahan & Yücel, 2012; Siddika et al., 2019; Su et al., 2015). The mechanical strength loss may be attributed to the loss of bonding between the rubber (due to smooth surface) and geopolymer matrix, loss of stiffness resulting from the rubber inclusions and decreased density with higher rubber incorporations. In addition, the results revealed that

the size of the crumb rubbers has no or very little influence on the mechanical strength since similar mechanical performance was taken when the similar percentage crumb rubbers were utilised. This may be due to the low size difference between the rubber particles, and also low rubber content (10% and 15%) replacements. However, in literature, there is a controversy regarding the influence of rubber sizes on mechanical performance. Some investigations stated that samples having finer rubber exhibited poor mechanical properties (Jafari & Toufigh, 2017; Siddika et al., 2019; Su et al., 2015), whereas others reported that coarse rubber incorporated samples showed better mechanical properties (Albano et al., 2005; Skripkiūnas et al., 2009). In this study, 10% tyre rubber incorporated (GB-TCR/10) samples showed slightly higher compressive strength, flexural strength and modulus of elasticity values than the 10% fine and coarse crumb rubber incorporated (GB-FCR/5.0-CCR/5.0) samples. The slightly better performance in the samples having larger rubber particles may be attributed to the higher particle bridging capacity of larger rubber particles than the finer ones. It was reported that no particle bridging is found due to the small size of crumb rubbers and particle bridging is dominant for the larger rubber particles (Sallam et al., 2008). Also, tyre rubber fibre orientation for the improved stress transfer may also be another factor for the better mechanical strength.

The SF incorporation significantly enhanced all mechanical strengths of the rubberised SCAAC specimens, except for marginal increase in compressive strength. The SF incorporation mitigated the negative effect of the rubbers in compressive strengths, whereas totally eliminated and even enhanced the modulus of elasticity, splitting tensile strength and flexural strength compared to reference specimens. A similar result that adding 1% SF into rubberised concretes enhanced the elasticity modulus, compressive strength and splitting tensile strength was stated in a previous study (Eisa et al., 2020). Also, splitting tensile strength and flexural strength enhancements were also reported due to the SF addition (Gülşan et al., 2019; Islam et al., 2017). The strength enhancement can be attributed to the hydrophilic properties of SFs (Ranjbar et al., 2016), enhancing the bond between matrix and SF. In addition, SFs due to the higher elastic modulus make easier the stress distribution so that tensile crack formation is restrained, enhancing the mechanical performances (Ismail & Hassan, 2017; Niş et al., 2021). Another reason of the mechanical strength improvements due to SF may be due to the enhanced bond strength resulting from the crack arresting capability of SF (Gülşan et al., 2019).

3.3. Scanning electron microscope analyses

Figure 3 presents the scanning electron microscope (SEM) micrographs for the rubberised specimens. The results revealed that the well-distributed geopolymeric pastes containing less unreacted slag particles show the denser and homogeneous microstructures of the SF-reinforced rubberised specimens. The crumb rubbers and SF could also be seen on the SEM micrographs. Meanwhile, wider interconnected macrocracks were observed at rubber–paste interface and matrix in the micrographs due to the self-drying and water evaporation (Wardhono et al., 2017), and shrinkage of the reaction products (Lee et al., 2014). Also, these cracks may be resulted from the high elasticity, deformability and also softness of the rubbers compared to matrix (Abdelmonem et al., 2019). These wider microcracks may cause loss of bonding between the geopolymeric matrix and the rubbers, resulting in a reduction in mechanical strengths. Similar findings were also reported from the SEM observations in the earlier investigation that the presence of voids and cracks in the cement paste/rubber interface shows a weak bonding condition (Abdelmonem et al., 2019; Thomas & Gupta, 2016). Figure 3(a) micrograph shows the N-(C)-A-S-H based geopolymerisation products without SF and rubbers. In Figure 3(b,c), the crumb rubber (CR) and tyre rubber (TCR) were clearly observed, and the macrocracks formed at the matrix phase due to self-drying, water evaporation and shrinkage of the reaction products. Meanwhile, Figure 3(d,e) micrographs illustrate the SF (shown as SF1), crumb rubber and tyre rubber with interconnected macrocracks in the geopolymer matrix. The weak interfacial transition zone (ITZ) between SF, matrix and rubbers was observed due to the existence of wider macrocracks, resulting in poor adherence. When steel fibrous micrographs were compared, specimens with coarser rubbers showed more porous microstructure (Figure 3(e)) with a high amount of macrocracks in the matrix compared with the micrograph of the specimen having finer rubbers (Figure 3(d)). The impact performance of steel fibrous specimens was adversely influenced by the weak ITZ between SFs and rubber–matrix composite. Also, it should be noted that the bond strength at the ITZ between SF and matrix is the weakest link in steel fibrous composites. The slightly lower impact performance of steel fibrous specimens with coarser rubbers may be attributed to the increased porosity

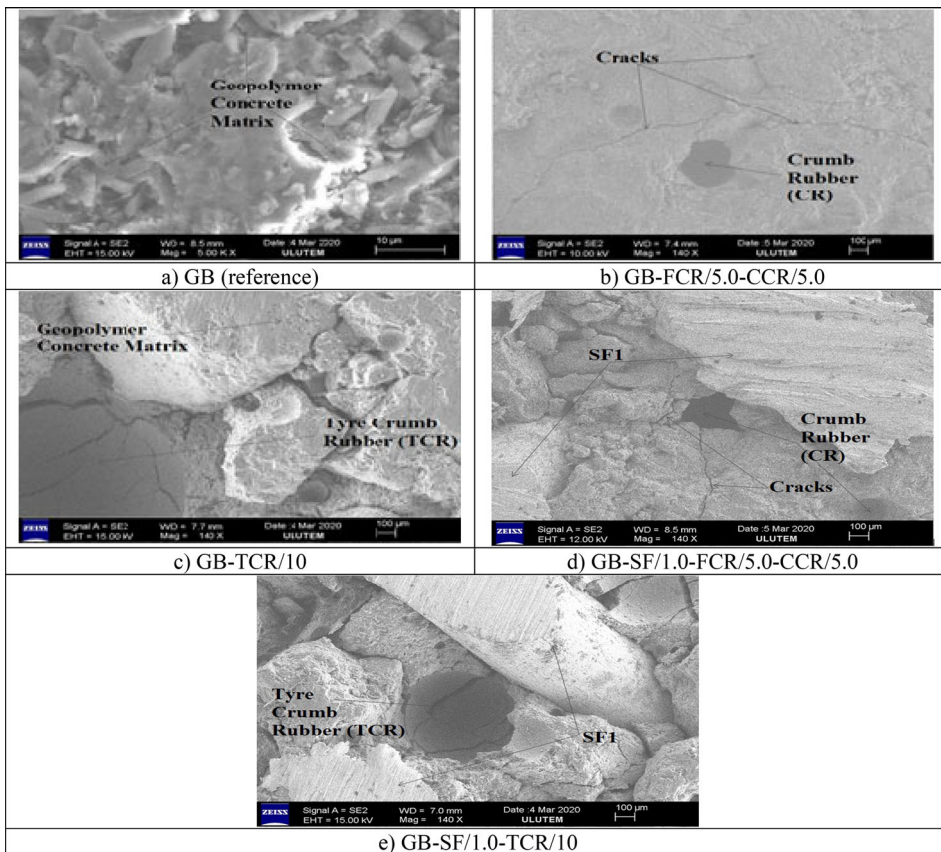


Figure 3. SEM micrographs of rubberised specimens.

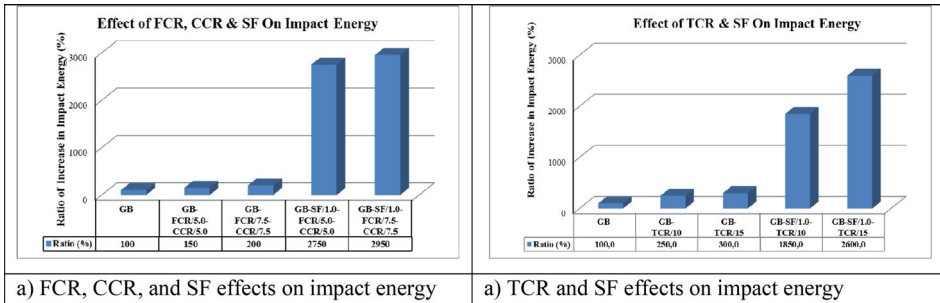
and low adherence due to porous microstructure and weak ITZ between SFs and rubber–matrix composite, which will be explained later.

3.4. Impact energy under drop weight test

The impact resistance of the rubberised SCAAC beam specimens was also determined using the drop-weight tests, and the results are given in Table 6. The failure number of blows was found as 2, 3, 4, 5 and 6 for GB (reference), GB-FCR/5.0-CCR/5.0, GB-FCR/7.5-CCR/7.5, GB-TCR/10, and GB-TCR/15 specimens, respectively. The crumb rubber incorporation improves the impact resistance and this enhancement was found more with higher crumb rubber replacements, which can be attributed to the low stiffness of crumb rubber particles. The results pointed out a decrease in the brittleness of SCAAC with an increase in the crumb rubber contents. A similar result was also reported in the previous study (Aly et al., 2019). In addition, the impact resistance enhanced with an enhancement in the crumb rubber size as TCR incorporated specimens showed better impact resistance than CCR and FCR incorporated specimens. A similar finding that the deformation and energy absorbing capacity increased with an increasing rubber sizes when the rubber contents kept constant was also reported (Liu et al., 2012). The failure number of blows was found as 55, 59, 37, and 52 for GB-SF/1.0-FCR/5.0-CCR/5.0, GB-SF/1.0-FCR/7.5-CCR/7.5, GB-SF/1.0-TCR/10, and GB-SF/1.0-TCR/15 specimens, respectively. The results pointed out that SF utilisation significantly enhanced the impact resistance. The impact energies of the GB-FCR/5.0-CCR/5.0, GB-FCR/7.5-CCR/7.5, GB-TCR/10, and GB-TCR/15 were found to be 1.5, 2, 2.5, 3 times higher than that of the reference concrete. The impact energy results indicated that 10% and 15% finer rubber (FCR and CCR) replacements enhanced the impact energy 1.5 times and 2 times, respectively. Meanwhile, 10% and 15% coarser rubber (TCR) replacements improved the impact energy 2.5 times and 3 times, respectively. The impact

Table 6. Drop-weight tests results.

Specimen	Drop number	Impactor weight (kg)	Drop height (cm)	Gravity (g) (m/s^2)	Impact energy (J)	Ratio on impact energy over (GB)
GB	2	28.5	10	9.81	55.917	1
GB-FCR/5.0-CCR/5.0	3	28.5	10	9.81	83.8755	1.5
GB-FCR/7.5-CCR/7.5	4	28.5	10	9.81	111.834	2
GB-TCR/10	5	28.5	10	9.81	139.7925	2.5
GB-TCR/15	6	28.5	10	9.81	167.751	3
GB-SF/1.0-FCR/5.0-CCR/5.0	55	28.5	10	9.81	1537.7175	27.5
GB-SF/1.0-FCR/7.5-CCR/7.5	59	28.5	10	9.81	1649.5515	29.5
GB-SF/1.0-TCR/10	37	28.5	10	9.81	1034.4645	18.5
GB-SF/1.0-TCR/15	52	28.5	10	9.81	1453.842	26


Figure 4. Impact energy variation due to the additions of crumb rubbers and SFs.

energy enhanced with an increase in the rubber replacement ratios, and the highest impact energy enhancements were obtained in the 15% rubber replacements. When the rubber types were compared, coarse rubber (TCR) incorporated specimens showed higher impact energy values than the finer rubber (FCR and TCR) incorporated specimens at both replacement ratios. The higher impact energy improvements in the coarser rubber (TCR) incorporated specimens can be attributed to the higher deformation and energy absorption capacity of coarser rubbers due to their more crack arresting (particle bridging) capability. A similar finding was also reported in the previous investigation (Liu et al., 2012).

Meanwhile, when SFs were incorporated, the impact energies of the GB-SF/1.0-FCR/5.0-CCR/5.0, GB-SF/1.0-FCR/7.5-CCR/7.5, GB-SF/1.0-TCR/10, and GB-SF/1.0-TCR/15 specimens were obtained as 27.5, 29.5, 18.5, and 26 times higher than the reference specimens (Figure 4). The 15% rubber incorporation enhanced the impact energy up to three times, and both 1% SF and 15% rubber incorporations significantly improved the impact energy up to 30 times for the SCAAC samples. The huge impact energy improvement results from the crack arresting capability of hooked end SFs, creating more adherence to the matrix, enabling higher stress transfer in between matrix and SF, thereby reducing the local or regional stresses (Niş et al., 2020).

In addition, the influence of rubber creates ductility so that more energy absorption capacities were obtained. In a previous investigation, it was claimed that rubbers create more flexibility to the rubber–matrix composite due to low stiffness, resulting in improved energy absorption capacity with an increase in rubber percentages (Gupta et al., 2015). In another study, the beneficial influences of crumb rubber replacements on improving the ductility and mechanical properties of concretes under impact loads were also reported. The 30% crumb rubber replacement improved the impact energy about three times compared to the reference concrete (Aly et al., 2019). In this study, further energy absorption capacity may be attributed to the increased crumb rubber and SF orientations in the casting direction due to SCC, resulting in superior flexural and impact performance. The contribution of SF on energy absorption capacity may be due to the pull-out behaviour and the bond strength since the energy absorption is generated mostly in the post-cracking zone and is related to the pull-out behaviour of the SF. The bond strength at the interface between SF and matrix is the weakest link in steel fibrous composites. Thus, the post-cracking behaviour is directly associated with the matrix properties and the amount of bonded area. The weaker matrices exhibit poor bonding properties than stronger ones. Similarly, for the same strength of matrices, the higher the bonded area (high SF volume or high SF aspect ratio), the more fibre pull-out resistance, resulting in better strength and energy absorption capacities (Liu et al., 2012).

When rubber sizes were considered, specimens with the coarser (TCR) rubbers showed higher energy absorption capacity than the specimens with the finer (FCR, CCR) rubbers for non-fibrous SCAAC. However, steel fibrous rubberised specimens with finer rubber sizes showed better energy absorption capacity than the coarser rubber sizes. It was reported that finer rubber particles exhibited better bonding performance than the coarser rubbers at all rubber replacement ratios (Gesoglu et al., 2015; Roychand et al., 2020). Also, the reduced rubber sizes provide larger specific surfaces and subsequently higher inter-particle frictions, resulting in a better bonding performance (AbdelAleem et al., 2018). However, in an earlier study, the performance of coarse rubbers in impact resistance was found significantly higher than the finer rubbers (Reda Taha et al., 2008). In the study, similar mechanical performances were taken for the samples having coarser and finer rubber particles. The high impact energy could be attributed to higher coarse rubber lengths for the specimens without SF. Meanwhile, more impact energy was obtained on the steel fibrous specimens with finer crumb rubbers, which can be attributed to larger specific surfaces and subsequently higher inter-particle frictions of finer rubbers reinforced with SF having higher pull-out resistance. For the non-fibrous specimens, the higher impact performance of specimens having coarser rubbers can be attributed to the crack arresting (particle bridging) capability of coarser rubbers, resulting in higher energy absorption capacity. However, when SFs were incorporated into the rubberised specimens, the crack bridging/crack arresting capability of SFs becomes more dominant than the rubbers. For this case (steel fibrous rubberised specimens), higher bond strength and reduced porosity are required for the higher impact resistance and energy. Therefore, the slightly lower impact performance of steel fibrous specimens with coarser rubbers may be attributed to the increased porosity and low adherence (poor bond) due to the porous microstructure and poor ITZ between SFs and rubber-matrix composite as explained in Figure 3(e).

3.5. Results of the drop-weight tests

In the study, the conditions of the specimens before the impact loading (left), after first drops (middle), and failure modes (right) are given in Figure 5. A thick flexural crack was observed at first drop and then failure emerged on the reference (control) samples at the 2nd impactor drop. The GB-FCR/5.0-CCR/5.0, GB-FCR/7.5-CCR/7.5, GB-TCR/10, and GB-TCR/15 specimens had a visible crack but the width of the crack was not as big as the reference specimens. The failure blows were found as 3, 4, 5, and 6 for GB-FCR/5.0-CCR/5.0, GB-FCR/7.5-CCR/7.5, GB-TCR/10, and GB-TCR/15 specimens, respectively. The measured displacements and crack widths before the failure were obtained as 0.007 mm and 0.5 mm for GB-FCR/5.0-CCR/5.0 specimens at 3rd drop, 0.0958 mm and 0.65 mm for GB-FCR/7.5-CCR/7.5 specimens at 4th drop, 0.1972 mm and 0.95 mm for GB-TCR/10 specimens at 5th drop, 0.079 mm and 5 mm for GB-TCR/15 specimens at 6th drop. The results pointed out that the crack widths of the FCR and CCR incorporated specimens were found low, and specimens with TCR/10 also showed a moderate crack width value (< 1 mm), whereas specimens with TCR/15 exhibited a high crack width value of 5 mm, showing that the failure occurred in a very ductile manner. The big crack width difference between TCR incorporated specimens with 10% and 15% replacements may be attributed to an inadequate number of TCR particles to arrest the opening of crack width at the failure spot for 10% replacement ratios. The results revealed that at least 15% of coarser rubber particles should be incorporated to obtain a reasonable energy absorption capacity. The slightly higher impact resistances with coarser rubber particles were also reported (Liu et al., 2012; Roychand et al., 2020).

When SFs were utilised with the recycled tyre rubbers, it was observed that SFs significantly improved the energy absorption capacities. The measured displacements and crack widths before the failure were obtained as 8.85 mm and 35 mm for GB-SF/1.0-FCR/5.0-CCR/5.0 specimens at 55th drop, 9.39 mm and 33 mm for GB-SF/1.0-FCR/7.5-CCR/7.5 specimens at 59th drop, 1.06 mm and 23 mm for GB-SF/1.0-TCR/10 specimens at 37th drop and, 2.56 mm and 19 mm for GB-SF/1.0-TCR/15 specimens at 52nd drop. The results pointed out that SF incorporation significantly improved the impact resistance, energy absorption capacity and ductility. The fibres bridge the cracks and keep the specimens in one piece and protect their integrity. The obtained results implied that the finer rubberised (FCR, CCR) specimens with SF showed better impact performance than the coarse rubberised (TCR) specimens with SF; however, the impact performance was found to be increased with an increase in rubber size when fibres were not utilised. The low impact performance with long rubbers could be attributed to the local bending of long rubbers (Yıldırım et al., 2020) and reduced bond strength with an increase in crumb rubber size (Hilal, 2017;

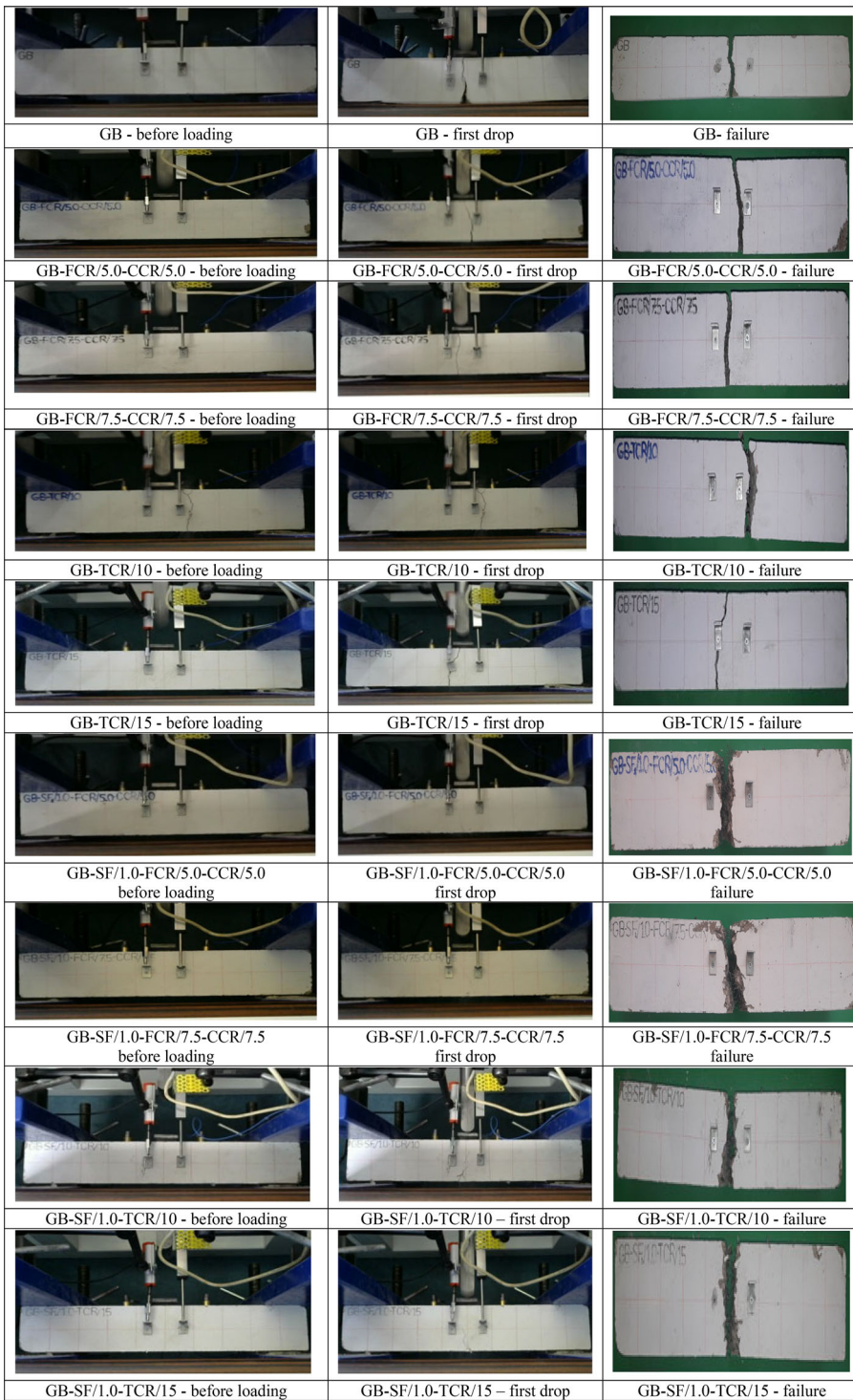


Figure 5. The drop-weights of SCGC Specimens (left: before loading, middle: after first drop, right: failure).

Roychand et al., 2020) between SF, matrix and rubbers. Also, the existence of SF and coarse rubbers caused voids in the matrix due to the inhomogeneous aggregate packing, resulting in a weaker matrix. The bond strength at the interface between SF and matrix is the weakest link, and weaker matrices show

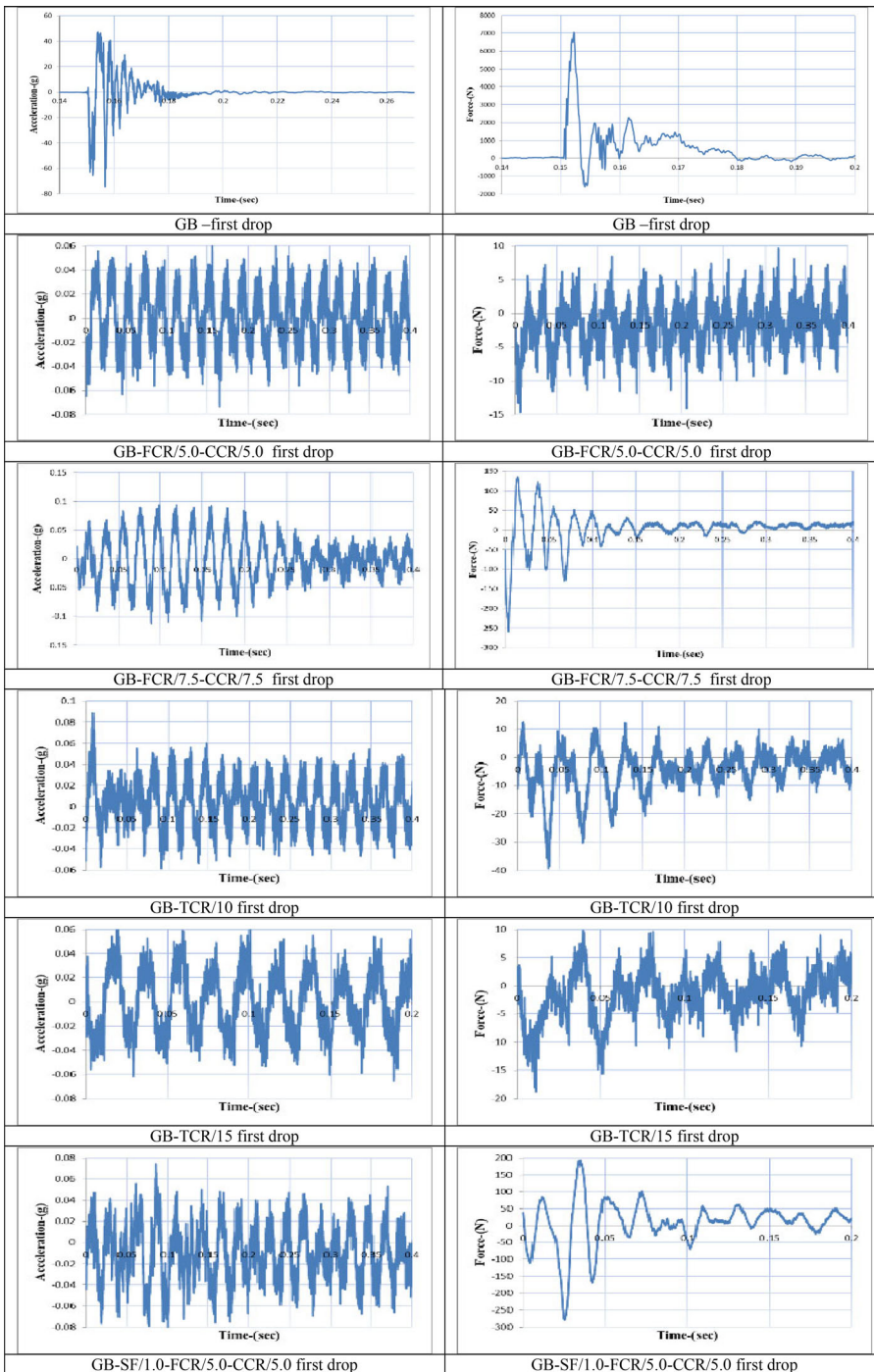


Figure 6. Average acceleration–time and force–time graphs for first drops.

poor bonding properties. The post-cracking behaviour is directly correlated with the bonded area and the matrix properties (Liu et al., 2012). Therefore, poor bonding properties due to coarser rubbers resulted in lower impact performance.

Figures 6 and 7 indicate the force–time graphs and acceleration–time graphs at first drops and failure drops. It was stated that acceleration–time results were found more appropriate than the velocity versus

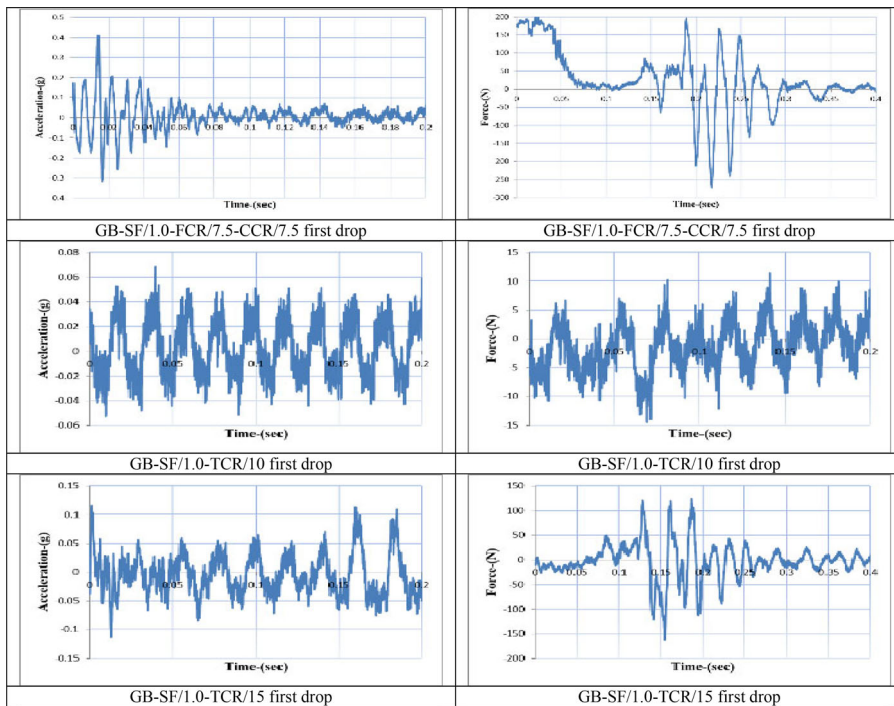


Figure 6. Continued.

time and displacement versus time graphs for the impact performance evaluations, and evaluations were commonly related to the acceleration values (Anil et al., 2015). In addition, velocity and displacement values were affected in a similar way to accelerations in the scope of the research. Therefore, impact assessments were made by acceleration–time graphs. The acceleration–time histories pointed out that beam specimens begin to vibrate with similar directions to the free-fall weights. The highest accelerations most of the time were reached in the first or second cycle. After the maximum accelerations, the beam specimens vibrate with decreasing amplitudes. Also, impact loads–time graphs were presented to evaluate the changes of impact loads with time. The findings showed that the impact loads influence the samples in a short time interval. The impact loads of non-fibrous rubberised specimens at failure were found lower than the impact loads of steel fibrous rubberised specimens, indicating very high damage for the specimens without SF. Meanwhile, the increase in the accelerations showed the increased resistance to impact loadings and enhanced absorbed energy capacities (Yılmaz et al., 2018), and lower accelerations caused lower velocity and displacement values (Anil et al., 2015). The highest acceleration value (between $-0.3g + 0.4g$) was obtained on the GB-SF/1.0-FCR/7.5-CCR/7.5 specimens, indicating the highest resistance against impact loads. The steel fibrous rubberised specimens showed slightly higher acceleration values ($\sim 0.1g$) than the rubberised specimens without SF, except for the GB-SF/1.0-TCR/10 ($\sim 0.05g$) specimens. Therefore, the GB-SF/1.0-TCR/10 specimens performed lower impact performance than the other specimens. The higher accelerations resulted in more crack widths and displacements values, indicating higher energy absorption capacity. The lower acceleration values observed on the non-fibrous rubberised specimens at both first and failure drops caused lower displacement and crack widths, resulting in lower energy absorption capacity and impact performance.

Figure 8 shows the maximum loads, maximum displacements and maximum crack widths measured after each drop and their relations of the only steel fibrous rubberised specimens since specimens without SF showed very poor crack widths and displacement values. Measured crack widths and displacements increased with an increase in the number of blows as shown in Figure 8(a,b). The results revealed that both crack width and displacement values of the steel fibrous rubberised specimens with finer (FCR, CCR) sizes were found to be significantly higher than the coarser rubber sized (TCR) rubberised specimens (Figure 8(c)). The lower impact performance of coarse rubbers can be attributed to the local bending (Yıldırım et al., 2020) and poor bond strength (Hilal, 2017; Roychand et al., 2020), and increased

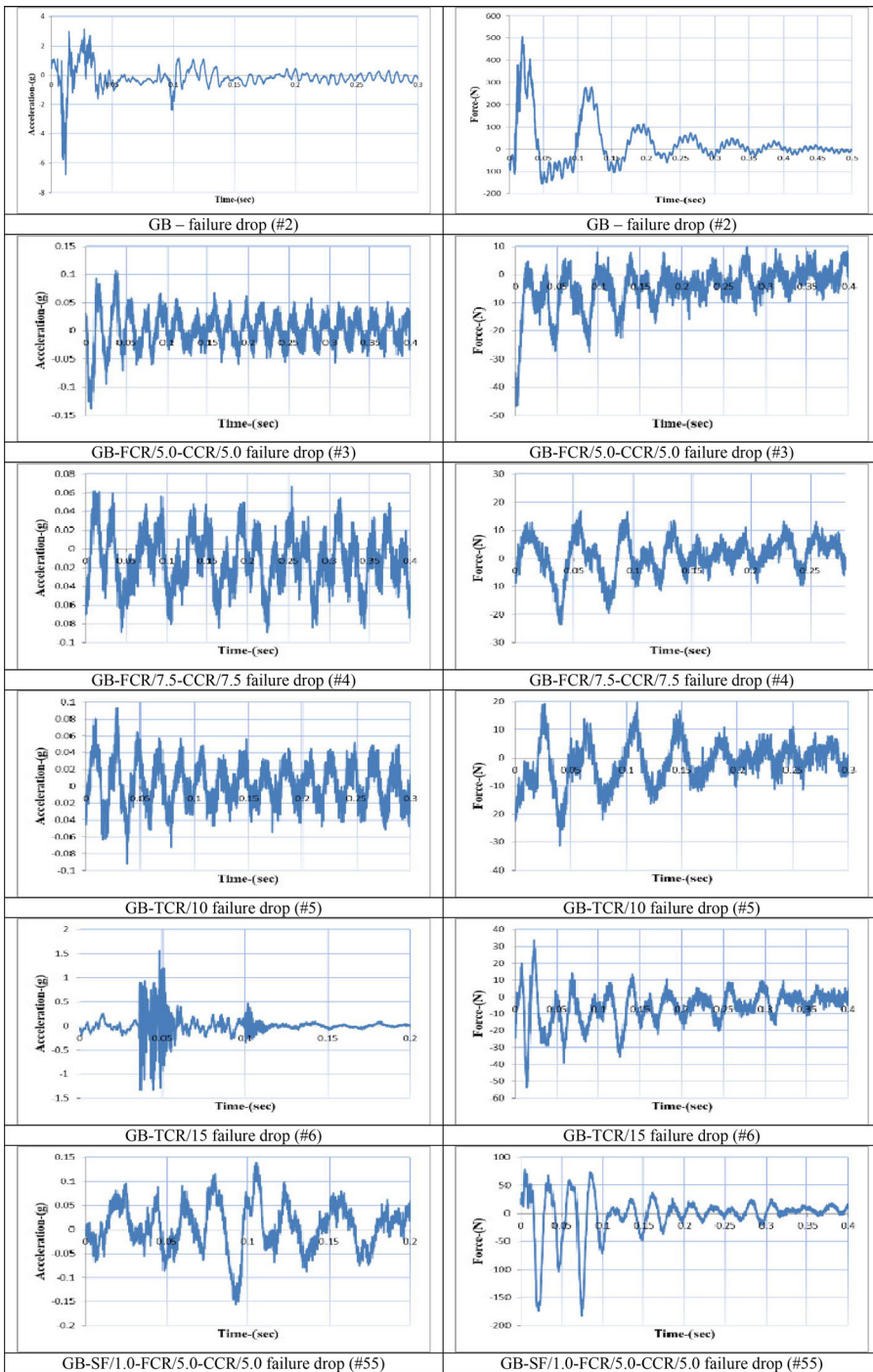


Figure 7. Average acceleration–time and force–time graphs for failure drops.

voids due to coarse rubber particles. The steel fibrous SCGC specimens with finer rubbers showed higher impact loads than the coarser ones and the impact resistance enhanced with the rubber replacements ratios. The ductility and energy absorption capacity of SCGC specimens under impact loads were significantly enhanced with an increase in the crumb rubber replacement ratio and SF utilisation. It should be noted that a fundamental crack was formed on the specimens after several impact loads. Then, SFs and

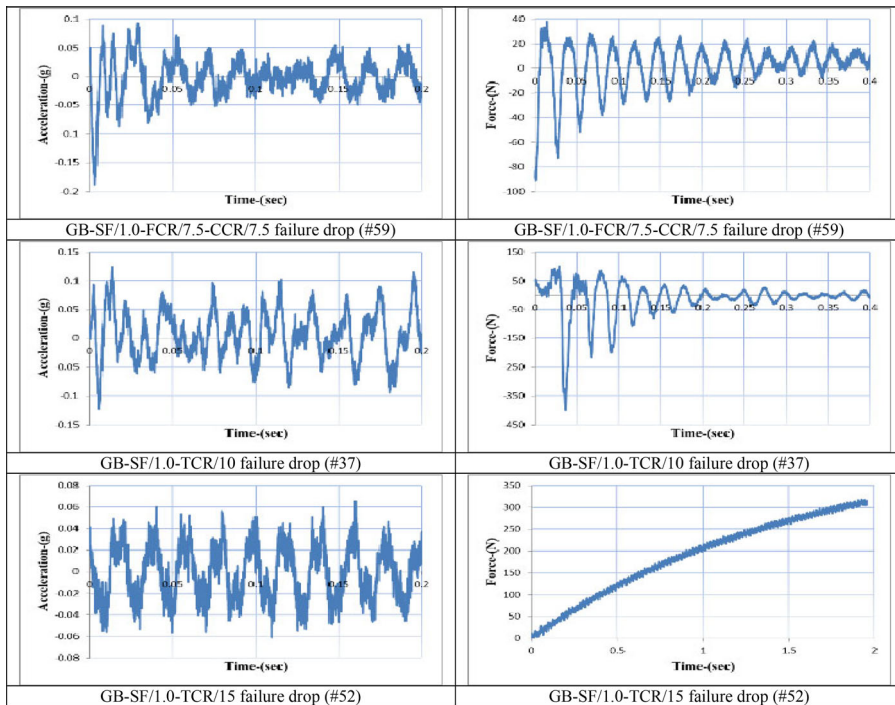


Figure 7. Continued.

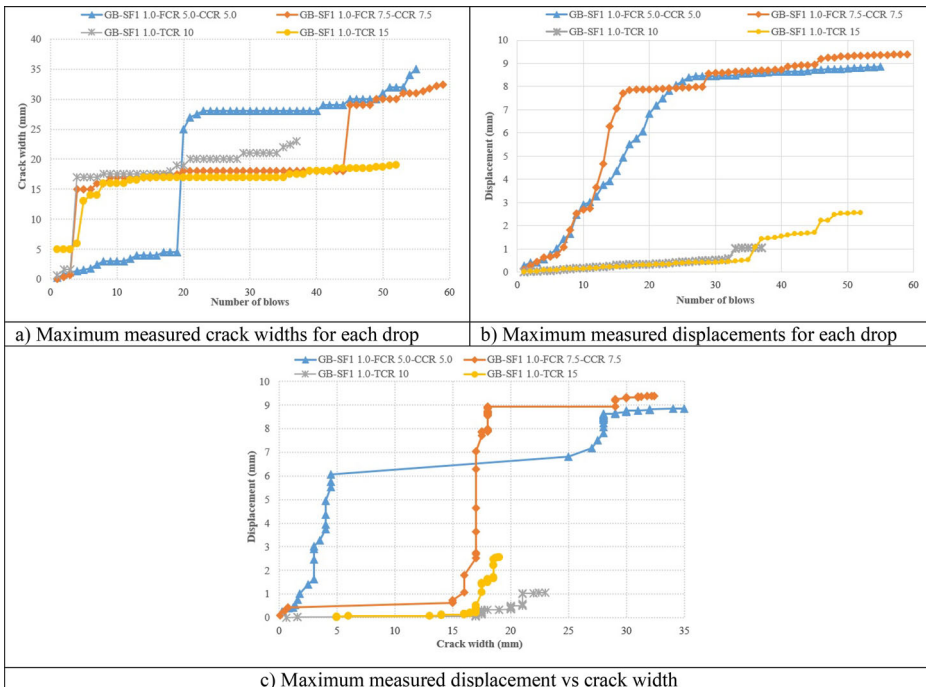


Figure 8. Maximum measured impact load, displacement, crack width relations under impact loads.

rubbers can provide a bridging effect to prevent microcracks from expansion, slowing down the propagation of cracks and the failure of specimens. This phenomenon was reflected by the stabilisation phase of the crack width values as shown in Figure 8.

4. Conclusions

In this study, the impact performances of the slag-based rubberised self-compacted alkali-activated concretes (SCAAC) with/without SF were evaluated. The fine and coarse crumb rubbers (FCR and CCR) were replaced by fine aggregates and tyre crumb rubbers (TCR) were replaced by coarse aggregates with replacement ratios of 10% and 15% to investigate the influence of rubber sizes, and rubber volume on the impact resistance and mechanical properties. The hooked end SF having a volume of 1% was also incorporated into the rubberised SCAAC specimens to investigate the combined effects of SF and rubbers on the resulting performances. The following conclusions were obtained in this research:

- The flowability and passing ability reduced with an increase in the crumb rubber percentage. The crumb rubbers with larger sizes (TCR) reduced the flowability and passing ability more than the finer rubber (FCR, CCR) sizes. Also, SF incorporation reduced fresh state performances further.
- The incorporation of crumb rubbers reduced the compressive strength, modulus of elasticity, splitting tensile strength and flexural strength of SCAAC specimens. The mechanical strength reduction was found to be more with an increase in the crumb rubber replacement ratio. Also, the size of the crumb rubbers (FCR, CCR or TCR) had no or very little influence on the mechanical strength results.
- The SF incorporation compensated the adverse effects of the rubbers on the mechanical strengths, and the mechanical strengths of all steel fibrous rubberised specimens were found to be better than non-fibrous rubberised and reference specimens, except for compressive strength (for reference only).
- The crumb rubber incorporations enhanced the impact resistance and this enhancement was found more with higher crumb rubber replacements. The impact energy of the specimens without SF slightly improved with an increase in the size of the rubbers. When SF was incorporated, the impact energy was significantly enhanced due to the crack arresting capability. The 15% rubber incorporation enhanced the impact energy up to three times, whereas both 1% SF and 15% rubber incorporation significantly improved the impact energy up to 30 times for SCAAC specimens.
- The crumb rubber size was found to be a significant parameter on the impact performance when SF was used. The coarse rubberised (TCR) samples with SF exhibited lower impact performance than the finer rubberised (FCR, CCR) specimens with SF, which can be attributed to the increased porosity and low adherence (poor bond) due to the porous microstructure and poor interfacial transition zone between SFs and rubber–matrix composite.
- The acceleration–time and force–time graphs indicated that the impact loads influence SCAAC samples in a very small time interval. Also, the impact loads of non-fibrous rubberised specimens at failure were found lower than the impact loads of steel fibrous rubberised specimens, indicating very high damage for the specimens without SF. The increase in the accelerations showed the increased impact performance, and the highest acceleration value was obtained on the GB-SF/1.0-FCR/7.5-CCR/7.5 specimens, indicating the highest impact resistance.
- The results revealed that crumb rubber utilisation in the form of aggregates as a sustainable construction material can be a solution to reduce the potential problems of waste tyres and OPC greenhouse gas emissions. The crumb rubbers and SFs should be utilised together in constructional applications to reduce the impact damages.

Acknowledgement

The raw/processed data required to reproduce these findings cannot be shared at this time as the data also forms part of an ongoing study.

Disclosure statement

No potential conflict of interest was reported by the authors.

Funding

The study was supported by Gaziantep University Scientific Research Project Coordination Units under project number MF. DT. 17. 06.

References

- AbdelAleem, B. H., Ismail, M. K., & Hassan, A. A. (2018). The combined effect of crumb rubber and synthetic fibers on impact resistance of self-consolidating concrete. *Construction and Building Materials*, 162, 816–829. <https://doi.org/10.1016/j.conbuildmat.2017.12.077>
- Abdelmonem, A., El-Feky, M. S., Nasr, E. S. A., & Kohail, M. (2019). Performance of high strength concrete containing recycled rubber. *Construction and Building Materials*, 227, 116660. <https://doi.org/10.1016/j.conbuildmat.2019.08.041>
- Alam, I., Mahmood, U. A., & Khattak, N. (2015). Use of rubber as aggregate in concrete: a review. *International Journal of Advanced Structures and Geotechnical Engineering*, 4(02), 92–96.
- Albano, C., Camacho, N., Reyes, J., Feliu, J. L., & Hernández, M. (2005). Influence of scrap rubber addition to Portland I concrete composites: Destructive and non-destructive testing. *Composite Structures*, 71(3–4), 439–446. <https://doi.org/10.1016/j.compstruct.2005.09.037>
- Aly, A. M., El-Feky, M. S., Kohail, M., & Nasr, E. S. A. (2019). Performance of geopolymer concrete containing recycled rubber. *Construction and Building Materials*, 207, 136–144. <https://doi.org/10.1016/j.conbuildmat.2019.02.121>
- Alzebaree, R., Çevik, A., Mohammedameen, A., Niş, A., & Gülşan, M. E. (2020). Mechanical performance of FRP-confined geopolymer concrete under seawater attack. *Advances in Structural Engineering*, 23(6), 1055–1073. <https://doi.org/10.1177/1369433219886964>
- Alzebaree, R., Gulsan, M. E., Nis, A., Mohammedameen, A., & Cevik, A. (2018). Performance of FRP confined and unconfined geopolymer concrete exposed to sulfate attacks. *Steel and Composite Structures*, 29(2), 201–218.
- Alzebaree, R., Mawlod, A. O., Mohammedameen, A., & Niş, A. (2021). Using of recycled clay brick/fine soil to produce sodium hydroxide alkali activated mortars. *Advances in Structural Engineering*, 24(13), 2996–3009.
- Anil, Ö., Kantar, E., & Yilmaz, M. C. (2015). Low velocity impact behavior of RC slabs with different support types. *Construction and Building Materials*, 93, 1078–1088. <https://doi.org/10.1016/j.conbuildmat.2015.05.039>
- Atahan, A. O., & Yücel, A. Ö. (2012). Crumb rubber in concrete: Static and dynamic evaluation. *Construction and Building Materials*, 36, 617–622. <https://doi.org/10.1016/j.conbuildmat.2012.04.068>
- Bing, C., & Ning, L. (2014). Experimental research on properties of fresh and hardened rubberized concrete. *Journal of Materials in Civil Engineering*, 26(8), 04014040. [https://doi.org/10.1061/\(ASCE\)MT.1943-5533.0000923](https://doi.org/10.1061/(ASCE)MT.1943-5533.0000923)
- Çevik, A., Alzebaree, R., Humur, G., Niş, A., & Gülşan, M. E. (2018). Effect of nano-silica on the chemical durability and mechanical performance of fly ash based geopolymer concrete. *Ceramics International*, 44(11), 12253–12264. <https://doi.org/10.1016/j.ceramint.2018.04.009>
- Chan, C. W., Yu, T., Zhang, S. S., & Xu, Q. F. (2019). Compressive behaviour of FRP-confined rubber concrete. *Construction and Building Materials*, 211, 416–426. <https://doi.org/10.1016/j.conbuildmat.2019.03.211>
- Chen, S.-J., Su, H.-B., Chang, J.-E., Lee, W.-J., Huang, K.-L., Hsieh, L.-T., Huang, Y.-C., Lin, W.-Y., & Lin, C.-C. (2007). Emissions of polycyclic aromatic hydrocarbons (PAHs) from the pyrolysis of scrap tires. *Atmospheric Environment*, 41(6), 1209–1220. <https://doi.org/10.1016/j.atmosenv.2006.09.041>
- Davidovits, J. (1994). Global warming impact on the cement and aggregates industries. *World Resour. Rev*, 6, 263–278.
- Day, K. E., Holtze, K. E., Metcalfe-Smith, J. L., Bishop, C. T., & Dutka, B. J. (1993). Toxicity of leachate from automobile tires to aquatic biota. *Chemosphere*, 27(4), 665–675. [https://doi.org/10.1016/0045-6535\(93\)90100-J](https://doi.org/10.1016/0045-6535(93)90100-J)
- Dehdezi, P. K., Erdem, S., & Blankson, M. A. (2015). Physico-mechanical, microstructural and dynamic properties of newly developed artificial fly ash based lightweight aggregate – Rubber concrete composite. *Composites Part B: Engineering*, 79, 451–455. <https://doi.org/10.1016/j.compositesb.2015.05.005>
- Eisa, A. S., Elshazli, M. T., & Nawar, M. T. (2020). Experimental investigation on the effect of using crumb rubber and steel fibers on the structural behavior of reinforced concrete beams. *Construction and Building Materials*, 252, 119078. <https://doi.org/10.1016/j.conbuildmat.2020.119078>
- Ganjan, E., Khorami, M., & Maghsoudi, A. A. (2009). Scrap-tyre-rubber replacement for aggregate and filler in concrete. *Construction and Building Materials*, 23(5), 1828–1836. <https://doi.org/10.1016/j.conbuildmat.2008.09.020>
- Gesoglu, M., Güneyisi, E., Hansu, O., İpek, S., & Asaad, D. S. (2015). Influence of waste rubber utilization on the fracture and steel–concrete bond strength properties of concrete. *Construction and Building Materials*, 101, 1113–1121. <https://doi.org/10.1016/j.conbuildmat.2015.10.030>
- Gong, D., Nadolski, S., Sun, C., Klein, B., & Kou, J. (2018). The effect of strain rate on particle breakage characteristics. *Powder Technology*, 339, 595–605. <https://doi.org/10.1016/j.powtec.2018.08.020>

- Gülşan, M. E., Alzeebaree, R., Rasheed, A. A., Niş, A., & Kurtoğlu, A. E. (2019). Development of fly ash/slag based self-compacting geopolymer concrete using nano-silica and steel fiber. *Construction and Building Materials*, 211, 271–283. <https://doi.org/10.1016/j.conbuildmat.2019.03.228>
- Gupta, T., Sharma, R. K., & Chaudhary, S. (2015). Impact resistance of concrete containing waste rubber fiber and silica fume. *International Journal of Impact Engineering*, 83, 76–87. <https://doi.org/10.1016/j.ijimpeng.2015.05.002>
- Hilal, N. N. (2017). Hardened properties of self-compacting concrete with different crumb rubber size and content. *International Journal of Sustainable Built Environment*, 6(1), 191–206. <https://doi.org/10.1016/j.ijsbe.2017.03.001>
- Holmes, N., Browne, A., & Montague, C. (2014). Acoustic properties of concrete panels with crumb rubber as a fine aggregate replacement. *Construction and Building Materials*, 73, 195–204. <https://doi.org/10.1016/j.conbuildmat.2014.09.107>
- Islam, A., Alengaram, U. J., Jumaat, M. Z., Ghazali, N. B., Yusoff, S., & Bashar, I. I. (2017). Influence of steel fibers on the mechanical properties and impact resistance of lightweight geopolymer concrete. *Construction and Building Materials*, 152, 964–977. <https://doi.org/10.1016/j.conbuildmat.2017.06.092>
- Ismail, M. K., & Hassan, A. A. (2017). Shear behaviour of large-scale rubberized concrete beams reinforced with steel fibres. *Construction and Building Materials*, 140, 43–57. <https://doi.org/10.1016/j.conbuildmat.2017.02.109>
- Jafari, K., & Toufigh, V. (2017). Experimental and analytical evaluation of rubberized polymer concrete. *Construction and Building Materials*, 155, 495–510. <https://doi.org/10.1016/j.conbuildmat.2017.08.097>
- Khatib, Z. K., & Bayomy, F. M. (1999). Rubberized Portland cement concrete. *Journal of Materials in Civil Engineering*, 11(3), 206–213. [https://doi.org/10.1061/\(ASCE\)0899-1561\(1999\)11:3\(206\)](https://doi.org/10.1061/(ASCE)0899-1561(1999)11:3(206))
- Kurtoglu, A. E., Alzeebaree, R., Aljumaili, O., Nis, A., Gulsan, M. E., Humur, G., & Cevik, A. (2018). Mechanical and durability properties of fly ash and slag based geopolymer concrete. *Advances in Concrete Construction*, 6(4), 345.
- Lee, N. K., Jang, J. G., & Lee, H. K. (2014). Shrinkage characteristics of alkali-activated fly ash/slag paste and mortar at early ages. *Cement and Concrete Composites*, 53, 239–248. <https://doi.org/10.1016/j.cemconcomp.2014.07.007>
- Li, H. L., Xu, Y., Chen, P. Y., Ge, J. J., & Wu, F. (2019). Impact energy consumption of high-volume rubber concrete with silica fume. *Advances in Civil Engineering*, 2019, 1–11. <https://doi.org/10.1155/2019/1728762>
- Liu, F., Chen, G., Li, L., & Guo, Y. (2012). Study of impact performance of rubber reinforced concrete. *Construction and Building Materials*, 36, 604–616. <https://doi.org/10.1016/j.conbuildmat.2012.06.014>
- Liu, H., Wang, X., Jiao, Y., & Sha, T. (2016). Experimental investigation of the mechanical and durability properties of crumb rubber concrete. *Materials*, 9(3), 172. <https://doi.org/10.3390/ma9030172>
- Ma, K., Feng, J., Long, G., Xie, Y., & Chen, X. (2017). Improved mix design method of self-compacting concrete based on coarse aggregate average diameter and slump flow. *Construction and Building Materials*, 143, 566–573. <https://doi.org/10.1016/j.conbuildmat.2017.03.142>
- Nis, A. (2018). Mechanical properties of steel fiber reinforced self-compacting concrete. *International Journal of Engineering Technologies*, 4(1), 33–40. <https://doi.org/10.19072/ijet.340259>
- Niş, A., & Altındal, İ. (2021). Compressive strength performance of alkali activated concretes under different curing conditions. *Periodica Polytechnica Civil Engineering*, 65(2), 556–565.
- Niş, A., & Altındal, M. B. (2019). Mechanical strength degradation of slag and fly ash based geopolymer specimens exposed to sulfuric acid attack. *Sigma: Journal of Engineering & Natural Sciences/Mühendislik ve Fen Bilimleri Dergisi*, 37(3), 917–926.
- Niş, A., Eren, N. A., & Çevik, A. (2021). Effects of nanosilica and steel fibers on the impact resistance of slag based self-compacting alkali-activated concrete. *Ceramics International*, 47(17), 23905–23918. <https://doi.org/10.1016/j.ceramint.2021.05.099>
- Niş, A., Özyurt, N., & Özturan, T. (2020). Variation of flexural performance parameters depending on specimen size and fiber properties. *Journal of Materials in Civil Engineering*, 32(4), 04020054. [https://doi.org/10.1061/\(ASCE\)MT.1943-5533.0003105](https://doi.org/10.1061/(ASCE)MT.1943-5533.0003105)
- Olivia, M., & Nikraz, H. (2012). Properties of fly ash geopolymer concrete designed by Taguchi method. *Materials and Design*, 36, 191–198. <https://doi.org/10.1016/j.matdes.2011.10.036>
- Pacheco-Torgal, F., Ding, Y., & Jalali, S. (2012). Properties and durability of concrete containing polymeric wastes (tyre rubber and polyethylene terephthalate bottles): An overview. *Construction and Building Materials*, 30, 714–724. <https://doi.org/10.1016/j.conbuildmat.2011.11.047>

- Park, Y., Abolmaali, A., Kim, Y. H., & Ghahremannejad, M. (2016). Compressive strength of fly ash-based geopolymer concrete with crumb rubber partially replacing sand. *Construction and Building Materials*, 118, 43–51. <https://doi.org/10.1016/j.conbuildmat.2016.05.001>
- Raffoul, S., Garcia, R., Pilakoutas, K., Guadagnini, M., & Medina, N. F. (2016). Optimisation of rubberised concrete with high rubber content: An experimental investigation. *Construction and Building Materials*, 124, 391–404. <https://doi.org/10.1016/j.conbuildmat.2016.07.054>
- Ranjbar, N., Talebian, S., Mehrali, M., Kuenzel, C., Metselaar, H. S. C., & Jumaat, M. Z. (2016). Mechanisms of interfacial bond in steel and polypropylene fiber reinforced geopolymer composites. *Composites Science and Technology*, 122, 73–81. <https://doi.org/10.1016/j.compscitech.2015.11.009>
- Reda Taha, M. M., El-Dieb, A. S., Abed El-Wahab, M. A., & Abdel-Hameed, M. E. (2008). Mechanical, fracture, and microstructural investigations of rubber concrete. *Journal of Materials in Civil Engineering*, 20(10), 640–649. [https://doi.org/10.1061/\(ASCE\)0899-1561\(2008\)20:10\(640\)](https://doi.org/10.1061/(ASCE)0899-1561(2008)20:10(640))
- Roychand, R., Gravina, R. J., Zhuge, Y., Ma, X., Youssf, O., & Mills, J. E. (2020). A comprehensive review on the mechanical properties of waste tire rubber concrete. *Construction and Building Materials*, 237, 117651. <https://doi.org/10.1016/j.conbuildmat.2019.117651>
- Sallam, H. E. M., Sherbini, A. S., Seleem, M. H., & Balaha, M. M. (2008). Impact resistance of rubberized concrete. *Engineering Research Journal*, 31(3), 265–271. <https://doi.org/10.21608/erjm.2008.69543>
- Siddika, A., Al Mamun, M. A., Alyousef, R., Amran, Y. M., Aslani, F., & Alabduljabbar, H. (2019). Properties and utilizations of waste tire rubber in concrete: A review. *Construction and Building Materials*, 224, 711–731. <https://doi.org/10.1016/j.conbuildmat.2019.07.108>
- Skripkiūnas, G., Grinys, A., & Miškinis, K. (2009). Damping properties of concrete with rubber waste additives. *Materials Science (Medžiagotyra)*, 15(3), 266–272.
- Su, H., Yang, J., Ling, T. C., Ghataora, G. S., & Dirar, S. (2015). Properties of concrete prepared with waste tyre rubber particles of uniform and varying sizes. *Journal of Cleaner Production*, 91, 288–296. <https://doi.org/10.1016/j.jclepro.2014.12.022>
- Thomas, B. S., & Gupta, R. C. (2016). Properties of high strength concrete containing scrap tire rubber. *Journal of Cleaner Production*, 113, 86–92. <https://doi.org/10.1016/j.jclepro.2015.11.019>
- Wallah, S. E., & Rangan, B. V. (2006). *Low-calcium fly ash-based geopolymer concrete: Longterm properties*. Curtin University of Technology.
- Wardhono, A., Gunasekara, C., Law, D. W., & Setunge, S. (2017). Comparison of long term performance between alkali activated slag and fly ash geopolymer concretes. *Construction and Building Materials*, 143, 272–279. <https://doi.org/10.1016/j.conbuildmat.2017.03.153>
- Wongsa, A., Sata, V., Nematollahi, B., Sanjayan, J., & Chindapasirt, P. (2018). Mechanical and thermal properties of lightweight geopolymer mortar incorporating crumb rubber. *Journal of Cleaner Production*, 195, 1069–1080. <https://doi.org/10.1016/j.jclepro.2018.06.003>
- Wu, Z., Shi, C., He, W., & Wu, L. (2016). Effects of steel fiber content and shape on mechanical properties of ultra-high performance concrete. *Construction and Building Materials*, 103, 8–14. <https://doi.org/10.1016/j.conbuildmat.2015.11.028>
- Yıldırım, G., Khiavi, F. E., Anıl, Ö., Şahin, O., Şahmaran, M., & Erdem, R. T. (2020). Performance of engineered cementitious composites under drop-weight impact: Effect of different mixture parameters. *Structural Concrete*, 21(3), 1051–1070. <https://doi.org/10.1002/suco.201900125>
- Yılmaz, T., Kıraç, N., Anıl, Ö., Erdem, R. T., & Sezer, C. (2018). Low-velocity impact behaviour of two way RC slab strengthening with CFRP strips. *Construction and Building Materials*, 186, 1046–1063. <https://doi.org/10.1016/j.conbuildmat.2018.08.027>
- Youssf, O., ElGawady, M. A., Mills, J. E., & Ma, X. (2014). An experimental investigation of crumb rubber concrete confined by fibre reinforced polymer tubes. *Construction and Building Materials*, 53, 522–532. <https://doi.org/10.1016/j.conbuildmat.2013.12.007>
- Zhang, W., Chen, S., & Liu, Y. (2017). Effect of weight and drop height of hammer on the flexural impact performance of fiber-reinforced concrete. *Construction and Building Materials*, 140, 31–35. <https://doi.org/10.1016/j.conbuildmat.2017.02.098>
- Zheng, L., Huo, X. S., & Yuan, Y. (2008). Strength, modulus of elasticity, and brittleness index of rubberized concrete. *Journal of Materials in Civil Engineering*, 20(11), 692–699. [https://doi.org/10.1061/\(ASCE\)0899-1561\(2008\)20:11\(692\)](https://doi.org/10.1061/(ASCE)0899-1561(2008)20:11(692))
- Zhong, H., Poon, E. W., Chen, K., & Zhang, M. (2019). Engineering properties of crumb rubber alkali-activated mortar reinforced with recycled steel fibres. *Journal of Cleaner Production*, 238, 117950. <https://doi.org/10.1016/j.jclepro.2019.117950>